2. M.A. Bezuglyi, N.V. Bezuglaya, S. Kostuk, «Influence of laser beam profile on light scattering by human skin during photometry by ellipsoidal reflectors», Devices and Methods of Measurements. 9(1):56–65, 2018.

3. Безуглий М.О. Особливості виготовлення еліпсоїдальних рефлекторів фотометрів / М.О. Безуглий, І.І. Синявський, Н.В. Безугла, А.Г. Козловський // Вісник НТУУ «КПІ». Серія Приладобудування, 2016. – № 2 (52). – С. 76–81.

4. Безуглий М.О. Контроль форми еліпсоїдальних рефлекторів біомедичних фотометрів / М.О. Безуглий, Лінючева О.В., Безугла Н.В., Бик М.В., Костюк С.А // Вісник НТУУ «КПІ». Серія Приладобудування, 2017. – № 1 (53). – С. 62–69.

5. Программы расчета оптических систем [Електронний ресурс]. – 2006. – Режим доступа к ресурсу: http:// optdesign.narod.ru/programs.htm.

6. M.A. Bezuglyi, N.V. Bezuglaya, I.V. Helich, «Ray tracing in ellipsoidal reflectors for optical biometry of media», Appl Opt., no. 56 (30), pp. 8520–8526, 2017.

7. Helich I.V. Features of aberrational analysis of ellipsoidal Reflectors to optical biomedical diagnostic / I.V. Helich. – Minsk, 2017.

УДК 621

CONTINUOUS-WAVE MICROCHIP LASER OPERATION OF Yb-DOPED GALLIUM GARNETS

J.M. Serres,[1] V. Jambunathan,[2] P. Loiko,[1,3] X. Mateos,[1,4] H. Yu,[5] H. Zhang,[5] J. Liu,[6] A. Lucianetti,[2] T. Mocek,[2] K. Yumashev,[3] U. Griebner,[4] V. Petrov,[4] M. Aguiló,[1] F. Díaz[1]

[1] *Física i Cristal·lografia de Materials i Nanomaterials, Universitat Rovira i Virgili, Tarragona, Spain*
[2] *HiLASE Centre, Institute of Physics CAS, Dolní Břežany, Czech Republic*
[3] *Center for Optical Materials and Technologies, Belarusian National Technical University, Minsk, Belarus*
[4] *Max Born Institute for Nonlinear Optics and Short Pulse Spectroscopy, Berlin, Germany*
[5] *State Key Laboratory of Crystal Materials, Shandong University, Jinan, China*
[6] *College of Physics, Qingdao University, Qingdao, China*

Ytterbium (Yb^{3+}) ions are attractive for high-power, efficient and wavelength-tunable laser operation near 1 μm. Yb-lasers enable power scaling due to a low quantum defect (Stokes shift) between the pump λp and laser λ wavelengths and because they can be pumped with commercially available, high-power InGaAs laser diodes emitting at 930–980 nm. The Yb^{3+} ion is also free of unwanted parasitic processes such as excited-state absorption and up-conversion and it typically shows very high luminescence quantum yield leading to exceptionally high laser efficiency (> 80%). One of the hosts for Yb^{3+} doping are the cubic ordered and disordered garnets. They possesses quite good thermo-optical and thermo-mechanical properties as well as relatively high thermal conductivity.

In the present report, we compare the microchip laser performance of a series of Yb-doped gallium garnets with ordered, Yb:$Y_3Ga_5O_{12}$ (Yb:YGG) and Yb:$Lu_3Ga_5O_{12}$ (Yb:LuGG) [1-3], as well as disordered, Yb:$Ca_3(Nb_{1.5}Ga_{0.5})Ga_3O_{12}$ (Yb:CNGG) and $Ca_3Li_yNb_{1.5+y}Ga_{3.5-2y}O_{12}$ (Yb:CLNGG) [4-6], crystal structure.

The Yb:LuGG and Yb:YGG crystals were grown in an oxygen atmosphere by the optical floating zone method, and Yb:CNGG and Yb:CLNGG ones were grown by the Czochralski method. From the as-grown bulks, rectangular samples were cut along the [111] crystallographic direction. Their thickness, aperture and doping level are specified in Table 1. The samples were wrapped with indium foil to improve the thermal contact and mounted in a water-cooled copper holder kept at ~12 °C.

Table 1. Compositional and Geometrical Parameters of the Studied Laser Crystals

Crystal	Doping, at.%	N_{Yb}, 10^{20} cm^{-3}	Thickness, mm	Aperture, mm^2
Yb:LuGG	7.13	9.4	6.00	3 × 3
Yb:YGG	7.35	9.7	6.02	3 × 3
Yb:CNGG	5.80	7.1	8.00	5 × 5
Yb:CLNGG	4.30	5.3	3.14	3 × 3

The microchip laser cavity consisted of a flat pump mirror (PM), AR coated for 0.9–1.0 μm and HR coated for 1.02–1.20 μm, and a set of flat output couplers (OC) with transmission T_{OC} = 1 %, 5 % or 10 % at the laser wavelength. The cavities contained no air gaps so that their lengths were equal to the geometrical length of the crystals. The fiber-coupled InGaAs diode was used, nominally emitting at around ~ 932. The pump beam was focused into the crystals with a lens assembly having a reimaging ratio of 1:1 and a focal length of 30 mm. The diode had a fiber core diameter of 105 μm and N.A. of 0.14. The diode provided a maximum output power of 25 W. The pump spot sizes in the focus w_p and confocal parameter $2z_R$ was then ~ 52 μm/1.0 mm. The crystals were pumped in a single-pass configuration.

The pump saturation intensity for the studied crystals was estimated to be ~ 20 kW/cm². For Yb:YGG, Yb:LuGG, and Yb:CNGG the pump absorption at high pump level was 60–70 % while for Yb:CLNGG it was ~ 50 % due to the shorter length of the crystal.

In Fig. 1, the absorption σ_{abs} and stimulated-emission cross-sections σ_{SE} spectra for the studied crystals are shown. The peak σ_{SE} values are slightly higher for Yb:YGG and Yb:LuGG (~ 2.6×10^{-20} cm^2) but Yb:CNGG and Yb:CLNGG provide broader emission bands (FWHM ~ 24 nm).

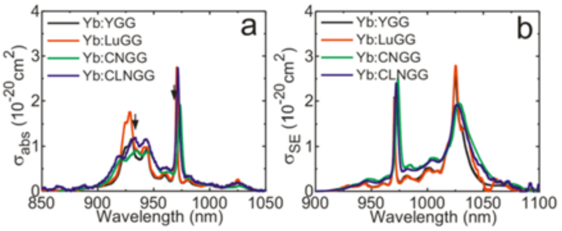

Fig. 1. Absorption (a) and stimulated-emission (b) cross-section spectra of the studied Yb-doped gallium garnets

Microchip laser operation was achieved with all garnets using the two described pump diodes. The input-output dependences for these lasers pumped at ~ 932 nm are shown in Fig. 2 with respect to the absorbed power. The Yb:LuGG crystal demonstrated superior laser performance. For T_{OC} = 10%, a maximum output power of 8.97 W was achieved at 1040 nm with a slope efficiency η = 75 %. The optical-to-optical efficiency was 63% and the laser threshold was at P_{abs} = 1.22 W. Using OCs with 5 % and 1 % transmission, the slope efficiency dropped to 69 % and 62 %, respectively.

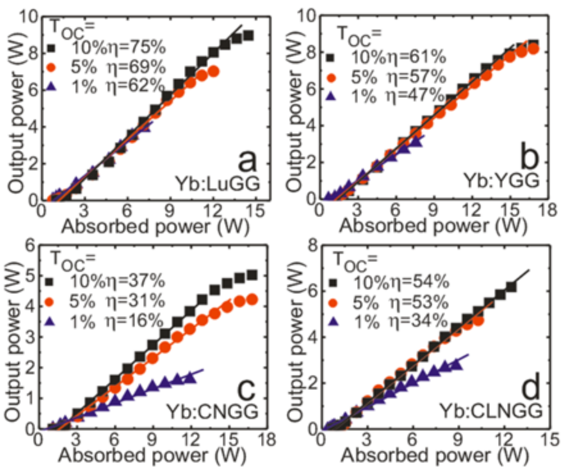

Fig. 2. Input-output dependences for microchip lasers based on Yb:LuGG (a), Yb:YGG (b), Yb:CNGG (c) and Yb:CLNGG (d) crystals. The pump wavelength is ~ 932 nm, η – slope efficiency

The Yb:YGG crystal showed slightly inferior laser performance. The maximum output power was 8.40 W at 1042 nm with η = 61% for T_{OC} = 10%. For Yb:CNGG and Yb:CLNGG microchip lasers, substantially lower output power was achieved. This decrease is attributed to the stronger thermo-optic effects in these crystals. The maximum output power generated with Yb:CLNGG was 6.1 W at 1039 nm with η = 54 % and with Yb:CNGG it was 5.1 W at 1051 nm with η = 37 % (both for TOC = 10 %).

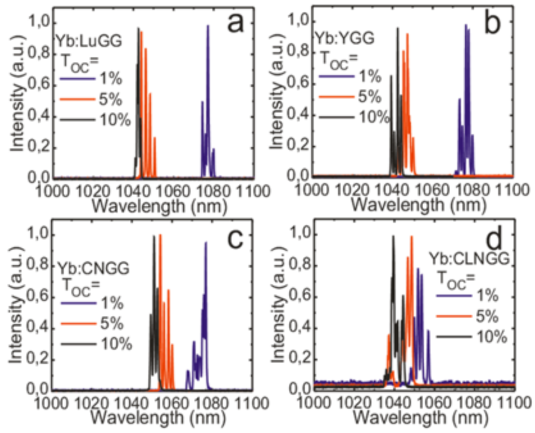

Fig. 3. Microchip laser emission spectra for Yb:LuGG (a), Yb:YGG (b), Yb:CNGG (c) and Yb:CLNGG (d) diode-pumped at 932 nm. The absorbed power is 7 W

For all crystals, thermal roll-over in the output dependences is observed. The range of P_{abs} corresponding to a linear input-output curve narrows at lower T_{OC}. For Yb:LuGG, Fig. 2(a), thermal roll-over starts at P_{abs} ~ 7, 11 and 13 W for T_{OC} = 1 %, 5 % and 10 %, respectively.

Typical laser emission spectra for all microchip lasers are shown in Fig. 3. All of them show a multi-peak behavior. For Yb:YGG and Yb:LuGG, the use of T_{OC} = 1 % corresponded to laser oscillation at ~ 1080 nm and with 5 % and 10 % OCs, laser emission occurred at ~ 1050 and 1040 nm, respectively. For Yb:CNGG and Yb:CLNGG, the shift of the emission wavelength was less pronounced. In the latter case, λ_l was ~ 1052, 1048 and 1039 nm fo$_{OC}$r T = 10 %, 5 % and 1 %, respectively.

The recorded laser emission spectra help to explain the peculiarities of the thermal rollover in the output dependences of the studied microchip lasers. The reason is a relatively high heat load under 932 nm pumping, as well as strongly localized heat deposition (as wp was only ~ 52 μm). In particular, for Yb:LuGG laser, the value of ηh estimated as Stokes shift, was 13.2 %, 10.9 % and 10.2 % for 1 %, 5 % and 10 % OC, respectively. Thus, stronger heat load is expected for lower T_{OC}, leading to a thermal roll-over at lower P_{abs}, as seen in Fig. 3.

The observed blue-shift of the laser wavelength with the increase of T_{OC} is typical for quasi-three-level Yb lasers and is explained with the gain cross-section, σg, spectra, Fig. 4. Here, $\sigma_g = \beta\sigma_{SE}-(1-\beta)\sigma_{abs}$ where β is the inversion ratio, $\beta = N_2/N_0$ where N_2 and N_0 are the number of ions excited in the upper laser level and overall number of ions, respectively. The gain spectra of Yb:LuGG, Yb:YGG and Yb:CNGG at very low β, typical for CW microchip lasers, are flat and very broad in the range from ~ 1060 to 1080 nm. For Yb:CLNGG, this range extends from 1040 to 1080 nm. With the increase of β, an absolute maximum is formed in the gain spectra and its position is shifting from 1045 to 1030 nm.

These spectral features are in good agreement with the recorded laser emission spectra, Fig. 3.

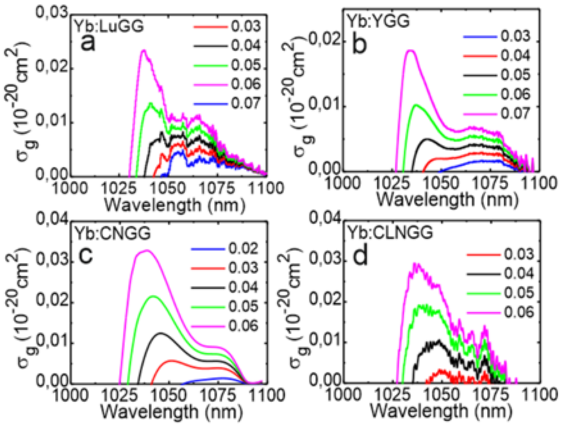

Fig. 4. Calculated gain cross-sections of Yb:LuGG (a), Yb:YGG (b), Yb:CNGG (c) and Yb:CLNGG (d) crystals for different inversion ratios *β*

References

1. W.Han, K. Wu, X. Tian, L. Xia, H. Zhang, and J. Liu, «Laser performance of ytterbium-doped gallium garnets: Yb:$Re_3Ga_5O_{12}$ (Re = Y, Gd, Lu)», Opt. Mater. Express 3(7), 920–927 (2013).

2. Y.Zhang, Z.Wei, Q.Wang, D. Li, Z. Zhang, H. Yu, H. Zhang, J. Wang, and L.Lv, «Diode-pumped efficient continuous-wave Yb:Y3Ga5O12 laser at 1035 nm», Opt. Lett. 36(4), 472–474 (2011).

3. Y. Zhang, Z. Wei, B. Zhou, C. Xu, Y. Zou, D. Li, Z. Zhang, H. Zhang, J. Wang, H. Yu, K. Wu, B. Yao, and J. Wang, «Diode-pumped passively mode-locked Yb:Y3Ga5O12 laser», Opt. Lett. 34(21), 3316–3318 (2009).

4. J.H. Liu, Y. Wan, Z. Zhou, X. Tian, W. Han, and H. Zhang, «Comparative study on the laser performance of two Yb-doped disordered garnet crystals: Yb:CNGG and Yb:CLNGG», Appl. Phys. B 109(2), 183–188 (2012).

5. J. Liu, W. Kong, X. Tian, Zh. Zhou, W. Han, Sh. Han, and H. Zhang, «Efficient laser oscillation of a new disordered Yb:CLNGG crystal», Laser Phys. Lett. 9(5), 394–397 (2012).

6. A. Schmidt, U. Griebner, H. Zhang, J. Wang, M. Jiang, J. Liu, and V. Petrov, «Passive mode-locking of the Yb:CNGG laser», Opt. Commun. 283(4), 567–569 (2010).